The effect of grain size of polycrystalline diamond on its heat spreading properties

Roland B. Simon[1], Julian Anaya[1], Firooz Faili[2], Richard Balmer[2], Gruffudd T. Williams[2], Daniel J. Twitchen[2], and Martin Kuball[1]

[1]*Center for Device Thermography and Reliability, HH Wills Physics Laboratory, University of Bristol, Tyndall Avenue, Bristol BS8 1TL, United Kingdom*

[2]*Element Six Technologies U.S. Corporation, Santa Clara, California 95054, USA*

The exceptionally high thermal conductivity of polycrystalline diamond (>20W/cmK) makes it a very attractive material for optimizing the thermal management of high-power devices. Herein, the thermal conductivity of a diamond sample capturing the grain size evolution from the nucleation towards the growth surface was studied by an optimized 3-omega technique. The thermal conductivity was found to decrease with decreasing grain size, in good agreement with theory. These results clearly indicate the minimum film thickness and the polishing thickness from nucleation needed to achieve the single-crystal diamond performance, and thus enable to get the optimal polycrystalline diamond for heat-spreading applications.

Polycrystalline diamond (PCD) components have been gaining popularity in recent years in industry and research due to the unparalleled properties of diamond, such as high hardness, transparency, and high thermal conductivity [1]. The growing range of applications includes thermal management (e.g. heat spreaders) for high-power electronics [2] and optics for X-ray lasers, high-power lasers, and gyrotrons [3, 4, 5]. Polycrystalline diamond is typically grown via chemical vapor deposition (CVD); the size and shape of grains, the concentration of defects, the quality of grain boundaries etc. are rather sensitive to the chemistry used in the growth reactor [6, 7, 8]. These factors determine the thermal conductivity of polycrystalline diamond, which ranges from a few W/mK up to 2500 W/mK [9]. Hence, to optimize the thermal performance of CVD diamond components, a thorough understanding of the mechanisms affecting its thermal conductivity is essential. CVD-PCD is a complex material, exhibiting a columnar grain structure with grain sizes expanding several orders of magnitude, increasing from the nucleation layer from the nanometer scale and through the material to the many-micrometer scale (see Fig.1.(a) and (b)). This gradient in the grain size strongly affects the phonon transport in the diamond, for instance it is known that the thermal conductivity of the first microns of CVD-PCD is 10-20 times lower than the bulk values.[9] Thus for maximizing the spreading of the heat in the PCD film, the diamond should be grown up to some thickness in which the grains are big enough to minimize its effect on the phonon flow. Besides,

the nucleation face should be polished to remove the small grain region which reduces the heat-spreading properties of the film. To optimize this process it is needed to correlate the local thermal conductivity with the grain structure of the sample, which has been typically circumvented by measuring samples of different thicknesses. [10] However this has limitations in accuracy as the measurements are not all performed on the same sample. Therefore, accurate local measurements are required to adequately describe and predict the PCD thermal properties. Measuring the thermal conductivity of diamond and other materials of high thermal conductivity with high accuracy generally poses significant challenges for the measurement instrumentation. Laser flash and hot bar techniques have been adapted for this purpose and enable measurement accuracies better than 10% [11, 12, 13]. However, these techniques measure the average thermal conductivity over large sample volumes in which the effect of the local grain structure is lost. In this letter, we show the local, grain size-dependent thermal conductivity along the growth direction with high accuracy on a specially designed diamond sample. This enables the extraction of the effect of grain size on the thermal conductivity of polycrystalline diamond, showing the minimum PCD thickness and polishing thickness needed to obtain similar heat-spreading performance than the more expensive and typically only 5-10mm size single crystal diamond. For this purpose, the 3-omega technique, which was originally designed for materials of lower thermal conductivity, has been extended from the typically used frequency range [14] to higher frequencies needed for high thermal conductivity materials.

To capture the effect of the grain size on the heat spreading properties of diamond films, a unique diamond sample with thickness of 290 µm and lateral dimensions of 20 mm by 20 mm was prepared by polishing both sides of a 2 mm thick CVD diamond slab at an angle of 5.9° as shown in Fig. 1(b). The resultant oblique-cut wafer exhibits a gradient in grain size in the lateral direction (x) while the grain size is constant in the other lateral direction (y). (Fig. 1(a)) The CVD diamond was grown following a commercial process recipe, which yields high-quality diamond exhibiting average bulk thermal conductivity values above 2000 W/mK for sample thicknesses above 600 µm [15]. The oblique-cut wafer was oxygen-terminated by ozone treatment, and a dense grid of 3-omega heaters was deposited via photolithography so that the heaters were perpendicular to the direction of the grain size gradient. The distance between the nearest heaters was 60 µm (Fig. 1(c)). The heaters consisted of a 50 nm Ti adhesion layer and 150 nm Pd layer with width of 10 µm and overall length of 1235 µm. This dense set allows the thermal conductivity of the sample to be probed with high spatial resolution, and in turn the dependence of the thermal conductivity on the grain size to be extracted with high accuracy. Since the measurements were performed on a single sample, this ensured that the results were not affected by sample-to-sample fluctuations occurring when multiple samples are grown in a reactor. The heaters were wire-bonded and the sample was placed in a Linkam THMS600 thermal stage for measurement in a temperature-controlled environment.

The 3-omega method applies a sinusoidal voltage of angular frequency ω to a metal line heater deposited on a sample, which gives rise to a temperature oscillation (ΔT) of angular frequency 2ω in the heater. This carries information about the thermal conductivity of the sample and it causes a 3ω component ($V_{3\omega}$) in the voltage drop along the line heater to emerge. The frequency-dependent $\Delta T(2\omega)$ in the heater can be derived from the measured $V_{3\omega}$ as:

$$V_{3\omega} = \frac{1}{2} V_0 \beta \Delta T(2\omega), \quad (1)$$

where V_0 is the ω component of the voltage drop along the heater and β is the temperature-resistance coefficient of the heaters, which has been calibrated for each measured heater separately.

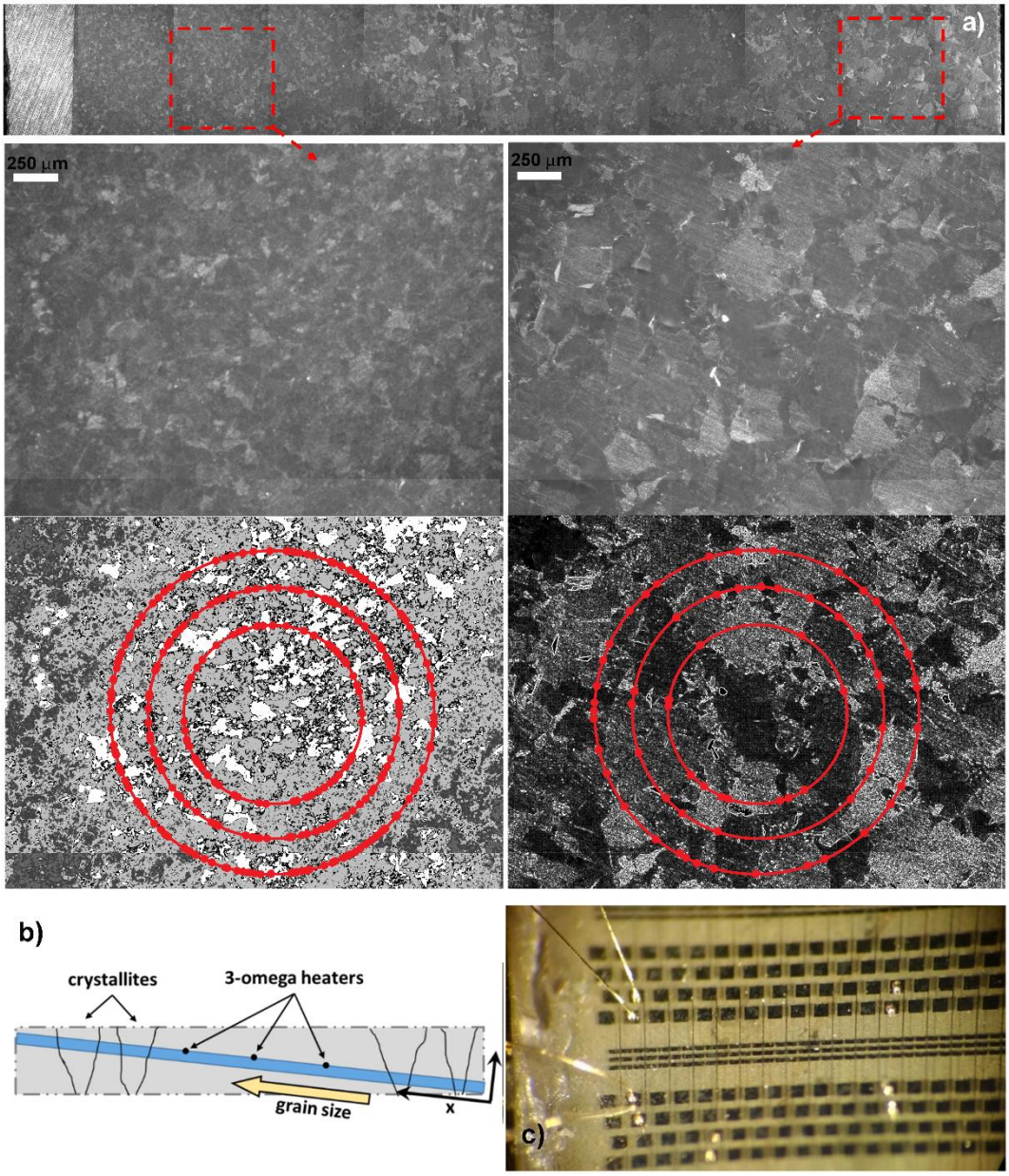

FIG. 1. (a) Optical micrographs showing crystalline structure of and the grain size gradient in the oblique cut diamond wafer. The local average grain size was determined by digitally enhancing the micrographs and counting the grain boundaries (marked by dots) intersecting a pattern consisting of 3 concentric circles, i.e. via the Abrams

method [20], as illustrated. (b) Schematic showing the structure of the 290 µm thick sample polished at 5.9 ° from a diamond slab. (c) 3-omega heater set covering the whole sample, showing one heater wire-bonded for measurement.

The $\Delta T(2\omega)$ generated in an infinitely long heater with half-width b, located on the surface of a sample of infinite thickness with thermal conductivity κ, and operated at RMS power p_{rms} is given by [14]:

$$\Delta T(2\omega) = \frac{p_{rms}}{\pi\kappa}\int_0^\infty \frac{\sin^2(\eta b)}{(\eta b)^2\sqrt{\eta^2+q(\omega)^2}}\,d\eta \tag{2}$$

$$q(\omega) = \frac{1}{\delta(\omega)} = \sqrt{\frac{2\omega\rho c_p}{\kappa}}, \tag{3}$$

where ω is the angular frequency, δ is the thermal penetration depth, c_p is the specific heat capacity, and ρ is the density of the sample. From Eq. 1, it is clear that $\Delta T(2\omega)$ is inversely proportional to the thermal conductivity and it is a monotonically decreasing function with ω, vanishing in the high frequency limit. When $\delta(\omega)$ is in the range: $d \gg \delta \gg b$, $\Delta T(2\omega)$ can be approximated with a linear function of $ln(\omega)$:

$$\Delta T(2\omega) \approx -\frac{p_{rms}}{2\pi\kappa}\left[ln(2\omega) + \ln\left(\frac{b^2\rho c_p}{\kappa}\right) - 2\xi\right] - i\frac{p_{rms}}{4\kappa} \tag{4}$$

where d is the thickness of the sample and ξ is a constant. Hence, in this frequency regime the thermal conductivity can be extracted with high accuracy via a simple linear fit of the measured ΔT *vs.* $ln(\omega)$, this is the so-called slope method [14]. In most reported studies using the 3-omega method, the excitation frequency range does not exceed a few kilohertz. However when the heat wave penetration depth is comparable to the thickness of the sample, i.e. the excitation frequency is lower than a critical value, the real temperature oscillation deviates from the one predicted by Eq. 4, and the accuracy of the thermal conductivity measurement is reduced. It is worth noting that the thermal penetration depth is proportional to the square root of the ratio of the thermal conductivity and the frequency as shown by Eq. 3, therefore Eq. 4 can be applied only to samples well above 250 µm-thick in the typically used frequency range for good quality diamond. Hence, higher frequencies are required for diamond; herein the 20-100 kHz range was used, corresponding to a probed depth of ~150 µm. The combination of high frequency and high thermal conductivity results in very low signal-to-carrier ratio, which is two orders of magnitude lower than for the usually measured 3-omega signals. This can cause significant measurement issues due to harmonic distortion of the electronics [16].

In order for the technique to operate in this low signal-to-carrier ratio scenario, the harmonic distortion has been minimized. This has been accomplished by using a signal generator with low

output distortion to provide the driving signal and a differential input stage with high common mode rejection ratio and low input distortion for subtracting signals from the heater and the reference resistor (inset of Fig. 2.). A Zürich Instruments HFLI lock-in amplifier was used for generating the driving signal, the subtraction, and for detecting the 3ω signal. To achieve a high common mode cancellation ratio, and to eliminate additional distortion produced by differential amplifiers present in traditional 3ω setups, a highly tunable Wheatstone bridge, consisting of only passive elements, was chosen over the differential amplifier configuration (inset of Fig. 2.) [17]. Resistors with a low thermal coefficient of resistance (±15 ppm/K) were chosen and the net resistance of the Wheatstone bridge was matched to the 50 Ω output impedance of the lock-in. The resistances of the arms of the Wheatstone bridge were equal, to minimize any phase differences due to the input capacitance of the lock-in. The ratio of Rh/R1 was chosen to be ~4:1, hence most of the power was dissipated in the heater. An R2 resistor, with resistance close to that of the 3-omega heater was connected in series with a 20-turn trimmer resistor (Rv), which enabled the fine balancing of the bridge, and hence ensured the high common mode cancellation ratio needed for measuring the diamond sample. The change in ΔT over the scanned frequency range was ~5-10 mK, and it exhibited a highly linear behavior in the frequency range used as displayed in Fig. 2. The uncertainty of the local thermal conductivity values determined via this method was less 8%, with the error arising mainly from residual harmonic distortion of the electronics.

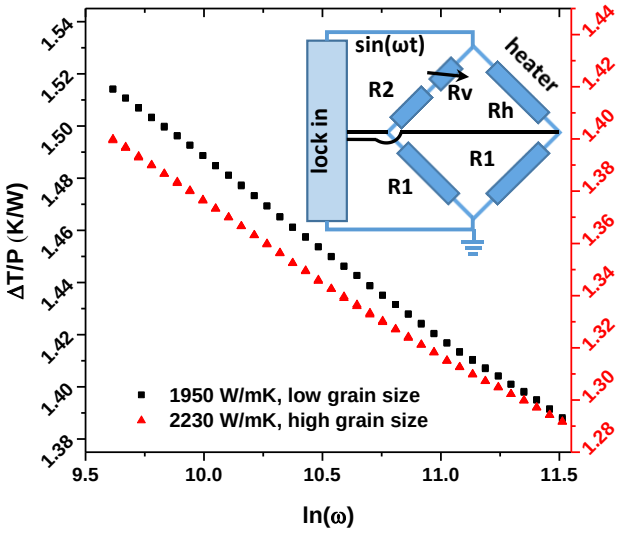

FIG. 2. Typical temperature change (ΔT) / electrical power (P) versus ln(ω) curves, with ω angular frequency, measured on the diamond sample; the gradient is inversely proportional to the thermal conductivity. Triangles corresponds to the region with larger grains (right axis), The inset shows a schematic of the Wheatstone bridge used for obtaining the 3-omega signal.

The thermal conductivities measured along the sample are shown in Fig. 3. There is an apparent decrease in the thermal conductivity from 2200 W/mK, i.e. single crystal values, in the region with large grain size to around 1900 W/mK in the region with smaller grains. The maximum values are thus close to what has been reported for II-a single crystal diamond. [18]

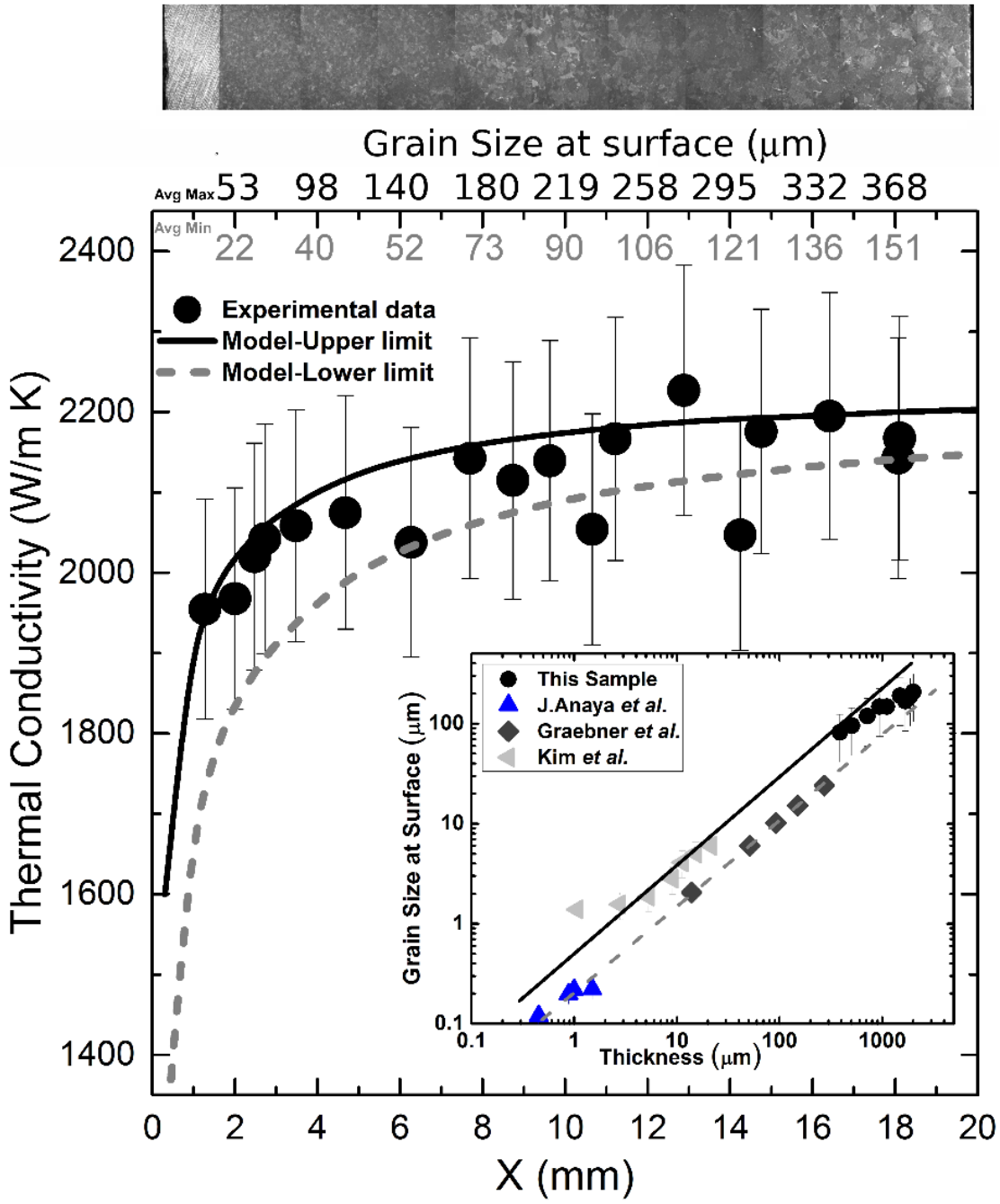

FIG. 3. Measured thermal conductivity (solid circles) as a function of lateral coordinate in the oblique-cut diamond wafer. The origin of the *x* axis corresponds to the low-grain-size edge of the wafer, see the micrograph aligned with the axis. Solid and dashed lines represent the thermal conductivity values predicted by a phonon scattering model using the estimated upper and lower limits of the thickness vs. surface grain size dependence shown in the inset. [9, 10, 21]

In order to gain further understanding of the observed thermal conductivity dependence measured along the diamond wafer, we analyzed the thermal conductivity of this sample by means of the phonon scattering model described in Ref. 9. This model can distinguish between the contributions from the different scattering mechanisms and the thermal conductivity is described as:

$$k(T, \Gamma, d, G) = \frac{k^C(T,\Gamma,d,)}{1+\frac{k^C(T,\Gamma,d,)}{d \times G}}, \quad (5)$$

where Γ is the parameter characterizing the quality of the lattice, which given the high thermal conductivity it can be assumed here equal to that of natural diamond, fully described my Morelli et al. [19]. This also means that the concentrations of dislocations, extended defects and vacancies are assumed to be negligible and the dominant scattering mechanisms are the isotope scattering and the grain boundary scattering. G is the thermal conductance between grains taken as the highest value reported in Ref. 9 (3 GW/m^{2}K). Finally, k^C is the intra-grain lattice thermal conductivity; calculated through the Callaway-Holland model detailed in Ref. 9 which includes the effect of grain boundary scattering. This phonon scattering mechanism is in principle frequency dependent, since some of the phonons are specularly scattered at the grain boundaries, depending on their frequency. However, this effect is only noticeable in diamond well below room temperature, and thus it is possible to assume a frequency independent grain boundary scattering in the investigated temperature range without loss of generality [20]. Therefore, under this approach the phonon grain boundary scattering rate can be described as $\tau_{gb}^i = \frac{L_{GS}}{v^i}$, where v^i is the sound velocity of each phonon branch and L_{GS} is a measure of the average mean free path between scattering events by grain boundaries. Given the columnar structure of this diamond, this distance can be characterized by the average lateral distance between grain boundaries, and thus by the lateral average grain size as described in Ref. 9. Therefore, in this simplified formalism there is no free parameter, and only the average grain size (d) and its evolution with the thickness – which can be obtained from the grain size at surface – is needed for this model to compare to the measured experimental data. Based on the optical micrographs, local average grain size over parts of the wafer were determined by the Abrams method [21]: after digital enhancement a pattern consisting three concentric circles of adequate radii was drawn on the images and the number of grain boundaries intersecting the pattern was counted (Fig. 1(a)), from which the average grain size at surface was calculated. However, at the low grain size side of the sample it was not possible to obtain a good quality micrograph due to the roughness of the sample backside and the low grain size, hence, the grain size measurement resulted in values with high uncertainty, as shown by the error bars in Fig. 3 inset. To circumvent this limitation, i.e. to obtain a more accurate grain size distribution over the whole sample, our grain size data was combined with the data reported in the literature on grain size at the surface vs diamond thickness. (Fig. 3, inset) [9, 19, 22]. A strong

correlation over three orders of magnitude in the grain size and thickness from the near nucleation region was observed, which also described the average lateral grain size evolution with the thickness. However, since the local grain size follows a rather broad distribution in our sample, as shown in the inset of Fig. 3, we determined an upper and lower limit for the grain size evolution rather than a single average trend. The predicted dependence of the thermal conductivity along the sample as a function of grain size is given in Fig. 3. Excellent agreement with the experimental data is observed regardless of whether the upper or lower limit of the grain size estimation is used in the thermal conductivity model. The results shown in Fig 3. accurately show the impact of the grain size at room temperature and above in samples with thickness of ≥100 μm, which are commonly used for heat sinking applications. Besides it is clear from Fig. 3 that to achieve the thermal conductivity of single crystal diamond (>20W/cmK), the diamond film should be thicker than 500 μm (corresponding to ~5mm in the lateral coordinate *x*) and therefore at least >220μm should be polished from the nucleation face for this particular material. Besides, the model enables to extrapolate the thermal conductivity below 100 μm, showing that for a diamond film of only 50 μm in thickness (non-polished) the thermal conductivity drops to 13-16 W/cmK, i.e. 60% of the single crystal thermal conductivity.

It is worth noting that in diamond at room temperature almost all the heat is carried by phonons with a mean free path smaller than 10 μm [23], as a consequence, the thermal conductivity reduction at room temperature and above only becomes significant when the grain size is reduced to below ~20 μm. This threshold however shifts to lower grain sizes at high temperatures as intra-grain scattering processes become dominant. On the other hand, the strength of grain boundary scattering would increase even for grain sizes well above 20 μm at cryogenic temperatures, and hence the grain-size dependence of the thermal conductivity would be significantly enhanced.

In conclusion, we shown the effect of grain size on thermal conductivity of CVD diamond films typically used as heat-spreaders by using an optimized low-noise 3 omega technique, which is also suitable for measuring other materials of high thermal conductivity. The experimental data compares well with a theoretical model describing the phonon scattering in CVD diamond, which also enabled to extrapolate the thermal conductivity below 100 microns in thickness, showing that for 50 mm thick PCD films the thermal conductivity is a 60% of the one observed in single crystal diamond. We also shown that to achieve the single crystal performance, the PCD film should be thicker than 500 μm and ~200μm should be removed from the nucleation face. These findings are important for the optimization of the growth, fabrication and thermal properties of heat spreaders and other CVD diamond components used in high power applications.

We acknowledge financial support from the Engineering and Physical Sciences Research Council (EPSRC). We thank our colleagues at Bristol, namely James W. Pomeroy and David Cussans for

their advice regarding the 3-omega electronics and Maire J. Power for proofreading of the manuscript. This work is in part supported by DARPA Contract No: FA8650-15-C-7517, monitored by Dr. Avram Bar Cohen and Dr. John Blevins supported by Dr. Joseph Maurer and Dr. Abirami Sivananthan. Any opinions, findings, and conclusions or recommendations expressed in this material are those of the authors and do not necessarily reflect the views of DARPA.

[1]R. S. Balmer, J. R. Brandon, S. L. Clewes, H. K. Dhillon, J. M. Dodson, I. Friel, P. N. Inglis, T. D. Madgwick, M. L. Markham, T. P. Mollart, N. Perkins, G. A. Scarsbrook, D. J. Twitchen, A. J. Whitehead, J. J. Wilman and S. M. Woollard, J. Phys.: Condens. Matter 21, 364221 (2009)

[2]J. W. Pomeroy, M. Bernardoni, D. C. Dumka, D. M. Fanning, and M. Kuball, Appl. Phys. Lett. 104, 083513 (2014)

[3]C. David, S. Gorelick, S. Rutishauser, J. Krzywinski, J. Vila-Comamala, V. A. Guzenko, O. Bunk, E. Färm, M. Ritala, M. Cammarata, D. M. Fritz, R. Barrett, R. Samoylova, J. Grünert, and H. Sinn, Sci. Rep. 1, article number: 57 (2011)

[4]E. Anoikin, A. Muhr, A. Bennett, D. Twitchen, and H. de Wit, Proc. SPIE 9346, Components and Packaging for Laser Systems, 93460T (February 20, 2015)

[5]G. Gantenbein, A. Samartsev, G. Aiello, G. Dammertz, J. Jelonnek, M. Losert, A. Schlaich, T. A. Scherer, D. Strauss, M. Thumm, and D. Wagner, IEEE Trans. Electron Devices 61, 1806 (2014)

[6]T. Lin, G. Y. Yu, A. T. S. Wee, Z. X. Shen, and Kian Ping Loh, Appl. Phys. Lett. 77, 2692 (2000)

[7]I.-D. Jeon, C. J. Park, D.-Y. Kim, and N. M. Hwang, J. Cryst. Growth 223, 6 (2001)

[8]H. Windischmann, Glenn F. Epps, Yue Cong, and R. W. Collins, J. Appl. Phys. 69, 2231 (1991);

[9]J. Anaya, S. Rossi, M. Alomari, E. Kohn, L. Tóth, B. Pécz, K. D. Hobart, T. J. Anderson, T. I. Feygelson, B. B. Pate, and M. Kuball, Acta Mater. 103, 141 (2016)

[10]J. E. Graebner, S. Jin, G. W. Kammlott, J. A. Herb, and C. F. Gardinier, Appl. Phys. Lett. 60, 1577 (1992)

[11]Y. Yamamoto, T. Imai, K. Tanabe, T. Tsuno, Y. Kumazawa, and N. Fujimori, Diamond Relat. Mater. 6, 105 (1997)

[12]R. H. Zhu , J. Y. Miao , J. L. Liu, L. X. Chen, J. C. Guo, C. Y. Hua, T. Ding, H. K. Lian, and C. M. Li, Diamond Relat. Mater. 50, 55 (2014)

[13]K. Belay, Z. Etzel, D. G. Onn, and T. R. Anthony, J. Appl. Phys. 79, (1996)

[14]D. G. Cahill, Rev. Sci. Instrum. 61, 802 (1990);

[15]S. Coe and R. Sussmann, Diamond Relat. Mater. 9, 1726 (2000).

[16]S. Ahmed, R. Liske, T. Wunderer, M. Leonhardt, R. Ziervogel, C. Fansler, T. Grotjohn, J. Asmussen, and T. Schuelke, Diamond Relat. Mater. 15, 389 (2006)

[17]F. L. Frank, V. Drach, and J. Fricke, Rev. Sci. Instrum. 64, 760 (1993)

[18]J. R. Olson, R. O. Pohl, J. W. Vandersande, A. Zoltan, T. R. Anthony, and W. F. Banholzer, Phys. Rev. B. 47, 14850 (1993)

[19]D. T.Morelli, J. P. Heremans, and G. A. Slack, Phys. Rev. B 66, 195304 (2002)

[20]J. W. Vandersande, Phys. Rev. B. 15, 2355 (1977)

[21]H. Abrams, Metallography 4, 59 (1971)

[22]J. G. Kim and J. Yu, Mat. Sci. Eng. B - Solid 57, 24 (1998)

[23]W. Li, N. Mingo, L. Lindsay, D. A. Broido, D. A. Stewart, and N. A. Katcho, Phys. Rev. B 85, 195436 (2012).